Proceedings of the Fifth Lunar Conference
(Supplement 5, Geochimica et Cosmochimica Acta)
Vol. 2 pp. 2005–2022 (1974)
Printed in the United States of America

Solar, spallogenic, and radiogenic rare gases in Apollo 17 soils and breccias

H. HINTENBERGER, H. W. WEBER, and L. SCHULTZ
Max-Planck-Institut für Chemie (Otto-Hahn-Institut), Mainz, Germany

Abstract—Concentration and isotopic composition of helium, neon and argon as well as ^{84}Kr and ^{132}Xe concentrations have been measured in Apollo 17 fines and breccias 72701, 74260, 75061, 75081, 79035, and 79135. From all samples, at least eight grain size fractions were analyzed and surface and volume correlated components determined. Ilmenite separates have been measured from the 35–54 μm fraction of 72701, 74241, 75081, and 79035.

^{21}Ne exposure ages for soils range from 27 m.y. (74220) to 230 m.y. (75081). The breccias, however, have exposure ages of about 600 m.y. (79035) and about 800 m.y. (79135). K–Ar ages for four soils lie between 2.9 and 3.9 b.y.

The trapped ^{4}He and ^{20}Ne concentrations in various soils are determined to a large degree by their ilmenite content. In ilmenite-rich material ($TiO_2 > 6\%$) correlations were found between the ^{4}He/^{36}Ar and ^{20}Ne/^{36}Ar ratios and the ^{36}Ar concentration, which is used as an indicator of the solar wind exposure. These ratios decrease with increasing solar wind exposure.

The concentrations of trapped ^{20}Ne and ^{36}Ar are correlated with the spallogenic ^{21}Ne. Furthermore, the trapped (^{4}He/^{3}He) ratios and the surface correlated (^{40}Ar/^{36}Ar) ratios appear to be correlated.

Characteristic differences in the rare gas abundance pattern have been found between breccias and soils.

(a) The concentrations of trapped gases as well as of spallogenic ^{21}Ne are higher in breccias than in soils.
(b) The ratio ^{132}Xe/^{36}Ar of the trapped gases in breccias is higher than in soils, indicating an excess of ^{132}Xe or a loss of ^{36}Ar and ^{84}Kr in breccias relative to soil materials.

In ilmenite the trapped He and Ne concentrations are higher than in bulk samples; the ^{36}Ar concentration, however, is for the three soils analyzed smaller in ilmenite than in the three bulk fines analyzed.

INTRODUCTION

THE CONCENTRATION PATTERN of surface correlated rare gas nuclides reflects—with the exception of ^{40}Ar—the abundance distribution of these isotopes in the solar wind. This pattern is, however, modified by various secondary processes acting on the lunar material such as diffusion losses, saturation effects, shock influences, or erosion phenomena. It is the aim of this investigation to elucidate the influence of these secondary processes on the elemental and isotopic composition of rare gases in lunar materials. Therefrom, information on the solar wind composition, on the history of soils and breccias, and on the mechanisms of the incorporation of rare gas nuclides into lunar materials can be obtained.

This paper reports on concentration and isotopic composition of He, Ne, and Ar as well as the concentration of ^{84}Kr and ^{132}Xe in bulk material, in grain size fractions of bulk material, and to some extent in ilmenite separates from soils and breccias of the Apollo 17 mission. It continues our earlier investigations on lunar material from the Apollo 11 to Apollo 16 missions (Hintenberger *et al.*, 1970a, 1970b, 1971; Hintenberger and Weber, 1973).

The samples investigated are listed in Table 1. They cover all major regolith types of the Apollo 17 landing site including the unique "orange" soil 74220 and the two gray soils collected adjacent to 74220. Furthermore, two dark matrix breccias have been analyzed. To increase the number of data points in the graphs and to verify that the relations found for Apollo 17 samples also hold for samples from other lunar missions, additional data from Hintenberger *et al.* (1970b, 1971) and Hintenberger and Weber (1971) are included in some figures. These samples and their abbreviations are listed in a footnote of Table 1.

EXPERIMENTAL PROCEDURES

The experimental details of the noble gas analyses have been described in earlier publications (Hintenberger *et al.*, 1970b, 1971; Schultz and Hintenberger, 1967; Weber, 1973).

At least eight grain size fractions from each of the six Apollo 17 soils and two breccias listed in Table 1 have been prepared by dry sieving. Stainless steel sieves of 20, 25, 35.5, 54, 75, 120, 200, and 300 μm, respectively, were used. In some cases, three smaller grain size fractions have been obtained using nylon sieves of 5 and 10 μm, respectively.

The ilmenite fractions were separated from bulk grain size fractions by Clerici solution in special glass vessels. The purity of these fractions was estimated from optical inspections to be better than 90% with the exception of the very small sample 72701 whose ilmenite content is only about 70%.

Table 1. Sample description[f].

Sample No. and description			K ppm	U ppm	Th ppm	TiO_2 %
7a	72701	light mantle surface soil	1330[a]	0.808[b]	2.962[b]	1.52[a]
7b	74220	"orange" soil	665[a]	0.161[c]	0.556[c]	8.81[a]
7c	74241	gray soils adjacent to 74220	1000[a]	0.14[d]	—	8.61[a]
7d	74260	gray soils adjacent to 74220	1000[a]	—	—	7.68[a]
7e	75061	dark mantle surface soils	630[a]	0.35[a]	0.89[a]	10.31[a]
7f	75081	dark mantle surface soils	670[a]	0.25[d]	—	9.41[a]
7G*	79035	dark matrix breccia (Van Serg Crater ejecta?)	—	0.31[e]	—	—
7H	79135	dark matrix breccia (interior of a boulder)	830[a]	—	—	5.15[a]

[a]LSPET (1973).
[b]Nunes *et al.* (1974).
[c]Tatsumoto *et al.* (1973).
[d]Jovanovic and Reed (1974).
[e]Morgan *et al.* (1974).
[f]In the figures other lunar samples are indicated by the following numbers: 10021 = 1A; 10060 = 1B; 10061 = 1C; 10084 = 1d; 10087 = 1e; 12070 = 2a; 14163 = 4a; 15471 = 5a; 68501 = 6a
*Note that numbers for breccias have a capital letter.

RESULTS

Bulk samples

Table 2 shows the results on bulk samples of Apollo 17 soils and breccias. Due to the heterogeneity of the samples and the small sample weights used the measured absolute concentrations vary far outside the analytical errors, which are in the order of ±3% for the concentrations of the He, Ne, and Ar isotopes and about ±10% for ^{84}Kr and ^{132}Xe. The precision of the data obtained have been tested by measurements on the Bruderheim standard. The concentrations given in Table 2 are mean values for the results obtained on different aliquots of the same sample. The number of aliquots measured and the maximum and minimum values observed for the ^{4}He contents are given in the last three lines. Table 2 includes also some elemental and isotopic abundance ratios.

Grain size fractions

The gas concentrations as well as the atomic and isotopic abundance ratios in grain size fractions of 72701, 74260, 75061, 75081, 79035, and 79135 are compiled in the Tables 3 to 8. The corresponding data for the orange soil 74220 and the

Table 2. Rare gas concentrations in cm^3 STP/g in bulk material of fines and breccias from Apollo 17 mission. Errors in isotope ratios 2%, errors in concentrations of He, Ne, and Ar about 3%, of Kr and Xe about 10%. Sample weights between 0.5–2.1 mg.

Nuclides and Ratios	72701,25	74220,47	74241,24	74260,9	75061,21	75081,72	79035,15	79135,32
^{3}He	2.81×10^{-5}	4.85×10^{-6}	4.91×10^{-5}	4.63×10^{-5}	4.14×10^{-5}	6.82×10^{-5}	6.68×10^{-5}	4.33×10^{-5}
^{4}He	8.07×10^{-2}	1.426×10^{-2}	1.573×10^{-1}	1.420×10^{-1}	1.086×10^{-1}	1.845×10^{-1}	1.882×10^{-1}	1.295×10^{-1}
^{20}Ne	1.664×10^{-3}	1.566×10^{-4}	1.542×10^{-3}	1.594×10^{-3}	1.248×10^{-3}	2.33×10^{-3}	3.10×10^{-3}	2.75×10^{-3}
^{21}Ne	4.27×10^{-6}	4.35×10^{-7}	3.98×10^{-6}	4.18×10^{-6}	3.26×10^{-6}	5.97×10^{-6}	8.48×10^{-6}	7.48×10^{-6}
^{22}Ne	1.292×10^{-4}	1.213×10^{-5}	1.228×10^{-4}	1.270×10^{-4}	9.47×10^{-5}	1.812×10^{-4}	2.42×10^{-4}	2.13×10^{-4}
^{36}Ar	3.81×10^{-4}	1.653×10^{-5}	1.593×10^{-4}	1.708×10^{-4}	1.676×10^{-4}	3.72×10^{-4}	4.10×10^{-4}	4.47×10^{-4}
^{38}Ar	7.24×10^{-5}	3.14×10^{-6}	3.06×10^{-5}	3.27×10^{-5}	3.17×10^{-5}	7.02×10^{-5}	7.84×10^{-5}	8.51×10^{-5}
^{40}Ar	4.15×10^{-4}	1.067×10^{-4}	1.197×10^{-3}	1.232×10^{-3}	1.565×10^{-4}	3.05×10^{-4}	9.19×10^{-4}	1.217×10^{-3}
^{84}Kr	2.0×10^{-7}	8.5×10^{-9}	7.2×10^{-8}	7.1×10^{-8}	9.4×10^{-8}	1.9×10^{-7}	1.9×10^{-7}	1.7×10^{-7}
^{132}Xe	2.2×10^{-8}	1.8×10^{-9}	1.5×10^{-8}	1.2×10^{-8}	1.2×10^{-8}	2.6×10^{-8}	4.4×10^{-8}	5.0×10^{-8}
^{4}He/^{3}He	2870	2940	3200	3070	2620	2710	2820	2990
^{20}Ne/^{22}Ne	12.88	12.91	12.56	12.55	13.18	12.86	12.92	12.91
^{22}Ne/^{21}Ne	30.3	27.9	30.9	30.4	29.0	30.4	28.5	28.5
^{36}Ar/^{38}Ar	5.26	5.26	5.21	5.22	5.29	5.30	5.22	5.24
^{40}Ar/^{36}Ar	1.089	6.45	7.51	7.21	0.934	0.820	2.24	2.73
^{4}He/^{20}Ne	48.5	91.1	102.0	89.1	87.0	79.2	60.7	47.1
^{20}Ne/^{36}Ar	4.37	9.47	9.68	9.33	7.45	6.26	7.56	6.17
^{36}Ar/^{84}Kr	1910	1940	2220	2410	1780	1960	2160	2620
^{84}Kr/^{132}Xe	9.1	4.7	4.7	5.9	8.1	7.3	4.3	3.4
number of aliquots	5	3	3	4	3	4	3	3
^{4}He-content								
max.	8.96×10^{-2}	1.458×10^{-2}	1.615×10^{-1}	1.442×10^{-1}	1.408×10^{-1}	2.02×10^{-1}	2.04×10^{-1}	1.712×10^{-1}
min.	7.03×10^{-2}	1.397×10^{-2}	1.530×10^{-1}	1.403×10^{-1}	7.10×10^{-2}	1.566×10^{-1}	1.630×10^{-1}	1.064×10^{-1}

Table 3. Rare gas concentrations in cm^3 STP/g in grain size fractions of fines from Apollo 17 sample 72701,25. Errors in isotope ratios 2%, errors in concentrations of He, Ne, and Ar about 3%, of Kr and Xe about 10%. Sample weights between 0.8–3.7 mg.

	<20 μm	20–25 μm	25–35 μm	35–54 μm	54–75 μm	75–120 μm	120–200 μm	200–300 μm
^3He	4.15×10^{-5}	1.789×10^{-5}	1.169×10^{-5}	7.23×10^{-6}	5.10×10^{-6}	4.02×10^{-6}	2.57×10^{-6}	3.00×10^{-6}
^4He	1.158×10^{-1}	5.08×10^{-2}	3.24×10^{-2}	1.967×10^{-2}	1.165×10^{-2}	9.33×10^{-3}	5.32×10^{-3}	6.66×10^{-3}
^{20}Ne	2.51×10^{-3}	1.240×10^{-3}	7.44×10^{-4}	4.77×10^{-4}	2.53×10^{-4}	2.09×10^{-4}	1.395×10^{-4}	1.839×10^{-4}
^{21}Ne	6.28×10^{-6}	3.32×10^{-6}	2.11×10^{-6}	1.497×10^{-6}	1.055×10^{-6}	8.45×10^{-7}	6.26×10^{-7}	7.37×10^{-7}
^{22}Ne	1.957×10^{-4}	9.60×10^{-5}	5.90×10^{-5}	3.83×10^{-5}	2.03×10^{-5}	1.695×10^{-5}	1.114×10^{-5}	1.482×10^{-5}
^{36}Ar	5.36×10^{-4}	2.54×10^{-4}	1.741×10^{-4}	1.115×10^{-4}	3.43×10^{-5}	4.65×10^{-5}	3.12×10^{-5}	4.65×10^{-5}
^{38}Ar	9.85×10^{-5}	4.83×10^{-5}	3.28×10^{-5}	2.14×10^{-5}	6.83×10^{-6}	8.91×10^{-6}	6.09×10^{-6}	8.99×10^{-6}
^{40}Ar	5.26×10^{-4}	2.96×10^{-4}	2.11×10^{-4}	1.601×10^{-4}	8.45×10^{-5}	1.130×10^{-4}	9.54×10^{-5}	1.315×10^{-4}
^{84}Kr	3.12×10^{-7}	1.46×10^{-7}	9.33×10^{-8}	6.17×10^{-8}	1.91×10^{-8}	2.48×10^{-8}	1.75×10^{-8}	2.59×10^{-8}
^{132}Xe	4.1×10^{-8}	1.92×10^{-8}	1.26×10^{-8}	9.5×10^{-9}	4.6×10^{-9}	4.1×10^{-9}	2.8×10^{-9}	4.3×10^{-9}
$^4He/^3He$	2790	2840	2770	2720	2280	2320	2070	2220
$^{20}Ne/^{22}Ne$	12.83	12.92	12.61	12.45	12.46	12.33	12.52	12.41
$^{22}Ne/^{21}Ne$	31.2	28.9	28.0	25.6	19.24	20.1	17.80	20.1
$^{36}Ar/^{38}Ar$	5.44	5.26	5.31	5.21	5.02	5.22	5.12	5.17
$^{40}Ar/^{36}Ar$	0.981	1.165	1.212	1.436	2.46	2.43	3.06	2.83
$^4He/^{20}Ne$	46.1	41.0	43.5	41.2	46.0	44.6	38.1	36.2
$^{20}Ne/^{36}Ar$	4.68	4.88	4.27	4.28	7.38	4.49	4.47	3.95
$^{36}Ar/^{84}Kr$	1720	1740	1870	1860	1800	1880	1780	1800
$^{84}Kr/^{132}Xe$	7.6	7.6	7.4	6.5	4.2	6.0	6.3	6.0

Table 4. Rare gas concentrations in cm^3 STP/g in grain size fractions of fines from Apollo 17 sample 74260,9. Errors in isotope ratios 2%, errors in concentrations of He, Ne, and Ar about 3%, of Kr and Xe about 10%. Sample weights between 0.5–2.9 mg.

	<20 μm	<20 μm	20–25 μm	25–35 μm	35–54 μm	75–120 μm	120–200 μm	200–300 μm
^3He	5.88×10^{-5}	5.80×10^{-5}	1.580×10^{-5}	1.364×10^{-5}	7.48×10^{-6}	5.93×10^{-6}	2.46×10^{-6}	6.91×10^{-6}
^4He	1.759×10^{-1}	1.745×10^{-1}	4.42×10^{-2}	3.86×10^{-2}	1.840×10^{-2}	1.454×10^{-2}	4.76×10^{-3}	1.997×10^{-2}
^{20}Ne	2.05×10^{-3}	2.10×10^{-3}	6.04×10^{-4}	4.84×10^{-4}	2.69×10^{-4}	1.626×10^{-4}	7.10×10^{-5}	2.22×10^{-4}
^{21}Ne	5.45×10^{-6}	5.40×10^{-6}	1.811×10^{-6}	1.531×10^{-6}	1.004×10^{-6}	7.24×10^{-7}	5.12×10^{-7}	8.20×10^{-7}
^{22}Ne	1.643×10^{-4}	1.688×10^{-4}	4.98×10^{-5}	4.04×10^{-5}	2.24×10^{-5}	1.364×10^{-5}	6.30×10^{-6}	1.905×10^{-5}
^{36}Ar	2.05×10^{-4}	2.25×10^{-4}	4.95×10^{-5}	4.66×10^{-5}	2.59×10^{-5}	1.727×10^{-5}	1.107×10^{-5}	2.90×10^{-5}
^{38}Ar	3.87×10^{-5}	4.34×10^{-5}	9.68×10^{-6}	9.16×10^{-6}	5.23×10^{-6}	3.55×10^{-6}	2.37×10^{-6}	5.66×10^{-6}
^{40}Ar	1.367×10^{-3}	1.588×10^{-3}	3.03×10^{-4}	3.08×10^{-4}	1.698×10^{-4}	1.353×10^{-4}	8.72×10^{-5}	2.29×10^{-4}
^{84}Kr	8.7×10^{-8}	8.8×10^{-8}	2.0×10^{-8}	1.9×10^{-8}	1.0×10^{-8}	6.4×10^{-9}	4.2×10^{-9}	1.3×10^{-8}
^{132}Xe	1.5×10^{-8}	1.7×10^{-8}	3.7×10^{-9}	2.3×10^{-9}	2.1×10^{-9}	1.2×10^{-9}	1.1×10^{-9}	2.2×10^{-9}
$^4He/^3He$	2990	3010	2800	2830	2460	2450	1935	2890
$^{20}Ne/^{22}Ne$	12.48	12.44	12.13	11.98	12.01	11.92	11.27	11.65
$^{22}Ne/^{21}Ne$	30.1	31.3	27.5	26.4	22.3	18.84	12.30	23.2
$^{36}Ar/^{38}Ar$	5.30	5.18	5.11	5.09	4.95	4.86	4.67	5.12
$^{40}Ar/^{36}Ar$	6.67	7.06	6.12	6.61	6.56	7.83	7.88	7.90
$^4He/^{20}Ne$	85.8	83.1	73.2	79.8	68.4	89.4	67.0	90.0
$^{20}Ne/^{36}Ar$	10.00	9.33	12.20	10.39	10.39	9.42	6.41	7.66
$^{36}Ar/^{84}Kr$	2350	2550	2540	2410	2560	2720	2640	2250
$^{84}Kr/^{132}Xe$	6.0	5.2	5.3	8.2	4.9	5.3	3.9	5.8

Table 5. Rare gas concentrations in cm^3 STP/g in grain size fractions of fines from Apollo 17 sample 75061,21. Errors in isotope ratios 2%, errors in concentrations of He, Ne, and Ar about 3%, of Kr and Xe about 10%. Sample weights between 0.75–2.8 mg.

	<20 μm	20–25 μm	25–35 μm	35–54 μm	54–75 μm	75–120 μm	120–200 μm	200–300 μm
^{3}He	5.55×10^{-5}	1.842×10^{-5}	1.443×10^{-5}	1.411×10^{-5}	6.46×10^{-6}	6.47×10^{-6}	8.19×10^{-6}	6.05×10^{-6}
^{4}He	1.532×10^{-1}	4.97×10^{-2}	3.94×10^{-2}	3.58×10^{-2}	1.416×10^{-2}	1.429×10^{-2}	1.940×10^{-2}	1.338×10^{-2}
^{20}Ne	2.07×10^{-3}	7.91×10^{-4}	6.60×10^{-4}	4.70×10^{-4}	2.80×10^{-4}	2.76×10^{-4}	2.62×10^{-4}	2.23×10^{-4}
^{21}Ne	5.44×10^{-6}	2.31×10^{-6}	2.04×10^{-6}	1.445×10^{-6}	1.083×10^{-6}	1.102×10^{-6}	8.79×10^{-7}	8.61×10^{-7}
^{22}Ne	1.657×10^{-4}	6.31×10^{-5}	5.45×10^{-5}	3.72×10^{-5}	2.23×10^{-5}	2.24×10^{-5}	2.11×10^{-5}	1.824×10^{-5}
^{36}Ar	2.80×10^{-4}	7.60×10^{-5}	6.78×10^{-5}	5.16×10^{-5}	2.59×10^{-5}	2.45×10^{-5}	3.47×10^{-5}	2.90×10^{-5}
^{38}Ar	5.33×10^{-5}	1.452×10^{-5}	1.320×10^{-5}	1.010×10^{-5}	5.02×10^{-6}	4.78×10^{-6}	6.71×10^{-6}	5.74×10^{-6}
^{40}Ar	2.62×10^{-4}	7.44×10^{-5}	7.26×10^{-5}	6.21×10^{-5}	3.73×10^{-5}	3.68×10^{-5}	5.41×10^{-5}	5.24×10^{-5}
^{84}Kr	1.64×10^{-7}	5.04×10^{-8}	4.13×10^{-8}	3.14×10^{-8}	1.33×10^{-8}	1.34×10^{-8}	2.01×10^{-8}	1.60×10^{-8}
^{132}Xe	2.3×10^{-8}	8.5×10^{-9}	1.3×10^{-8}	5.8×10^{-9}	2.2×10^{-9}	2.0×10^{-9}	2.9×10^{-9}	2.7×10^{-9}
^{4}He/^{3}He	2760	2700	2730	2540	2190	2210	2370	2210
^{20}Ne/^{22}Ne	12.49	12.54	12.11	12.63	12.56	12.32	12.42	12.23
^{22}Ne/^{21}Ne	30.5	27.3	26.7	25.7	20.6	20.3	24.0	21.2
^{36}Ar/^{38}Ar	5.25	5.23	5.14	5.11	5.16	5.13	5.17	5.05
^{40}Ar/^{36}Ar	0.936	0.979	1.071	1.203	1.440	1.502	1.559	1.807
^{4}He/^{20}Ne	74.0	62.8	59.7	76.2	50.6	51.8	74.0	60.0
^{20}Ne/^{36}Ar	7.39	10.41	9.73	9.11	10.81	11.27	7.55	7.69
^{36}Ar/^{84}Kr	1710	1510	1640	1640	1950	1830	1730	1810
^{84}Kr/^{132}Xe	7.1	5.9	3.1	5.4	6.0	6.7	6.9	5.9

Table 6. Rare gas concentrations in cm^3 STP/g in grain size fractions of fines from Apollo 17 samples 75081,72. Errors in isotope ratios 2%, errors in concentrations of He, Ne, and Ar about 3%, of Kr and Xe about 10%. Sample weights between 0.9–3.0 mg.

	<20 μm	20–25 μm	25–35 μm	35–54 μm	54–75 μm	75–120 μm	120–200 μm	200–300 μm
^{3}He	7.98×10^{-5}	2.62×10^{-5}	2.22×10^{-5}	1.876×10^{-5}	9.69×10^{-6}	1.008×10^{-5}	9.59×10^{-6}	8.06×10^{-6}
^{4}He	2.15×10^{-1}	7.25×10^{-2}	5.79×10^{-2}	5.01×10^{-2}	2.29×10^{-2}	2.40×10^{-2}	2.24×10^{-2}	1.907×10^{-2}
^{20}Ne	2.72×10^{-3}	1.035×10^{-3}	8.49×10^{-4}	6.81×10^{-4}	3.45×10^{-4}	3.04×10^{-4}	2.90×10^{-4}	2.42×10^{-4}
^{21}Ne	6.89×10^{-6}	3.00×10^{-6}	2.45×10^{-6}	2.05×10^{-6}	1.266×10^{-6}	1.107×10^{-6}	1.017×10^{-6}	9.00×10^{-7}
^{22}Ne	2.18×10^{-4}	8.12×10^{-5}	6.79×10^{-5}	5.39×10^{-5}	2.78×10^{-5}	2.43×10^{-5}	2.33×10^{-5}	1.946×10^{-5}
^{36}Ar	4.38×10^{-4}	1.247×10^{-4}	1.101×10^{-4}	9.90×10^{-5}	3.76×10^{-5}	3.49×10^{-5}	3.87×10^{-5}	3.78×10^{-5}
^{38}Ar	8.24×10^{-5}	2.43×10^{-5}	2.12×10^{-5}	1.935×10^{-5}	7.34×10^{-6}	7.11×10^{-6}	7.54×10^{-6}	7.53×10^{-6}
^{40}Ar	3.46×10^{-4}	1.155×10^{-4}	9.97×10^{-5}	1.039×10^{-4}	4.36×10^{-5}	4.08×10^{-5}	4.40×10^{-5}	5.42×10^{-5}
^{84}Kr	2.2×10^{-7}	7.8×10^{-8}	5.8×10^{-8}	6.2×10^{-8}	2.2×10^{-8}	2.1×10^{-8}	2.1×10^{-8}	2.3×10^{-8}
^{132}Xe	2.8×10^{-8}	1.0×10^{-8}	6.5×10^{-9}	8.4×10^{-9}	2.9×10^{-9}	3.2×10^{-9}	2.7×10^{-9}	2.8×10^{-9}
^{4}He/^{3}He	2690	2770	2610	2670	2360	2380	2340	2370
^{20}Ne/^{22}Ne	12.48	12.74	12.50	12.63	12.41	12.51	12.45	12.44
^{22}Ne/^{21}Ne	31.6	27.1	27.7	26.3	22.0	22.0	22.9	21.6
^{36}Ar/^{38}Ar	5.32	5.13	5.19	5.12	5.12	4.91	5.13	5.02
^{40}Ar/^{36}Ar	0.790	0.926	0.906	1.049	1.160	1.169	1.137	1.434
^{4}He/^{20}Ne	79.0	70.0	68.2	73.6	66.4	78.9	77.2	78.8
^{20}Ne/^{36}Ar	6.21	8.30	7.71	6.88	9.18	8.71	7.49	6.40
^{36}Ar/^{84}Kr	1960	1600	1900	1600	1710	1660	1840	1640
^{84}Kr/^{132}Xe	8.1	7.8	8.9	7.4	7.6	6.6	7.8	8.2

Table 7. Rare gas concentrations in cm^3 STP/g in grain size fractions of fines from Apollo 17 sample 79035,15. Errors in isotope ratios 2%, errors in concentrations of He, Ne, and Ar about 3%, of Kr and Xe about 10%. Sample weights between 0.6–3 mg.

	<20 μm	20–25 μm	25–35 μm	35–54 μm	54–75 μm	75–120 μm	120–200 μm	200–300 μm
^{3}He	9.11×10^{-5}	3.51×10^{-5}	2.57×10^{-5}	1.705×10^{-5}	1.346×10^{-5}	1.202×10^{-5}	9.15×10^{-6}	7.84×10^{-6}
^{4}He	2.71×10^{-1}	9.84×10^{-2}	7.21×10^{-2}	4.33×10^{-2}	3.18×10^{-2}	2.85×10^{-2}	2.05×10^{-2}	1.840×10^{-2}
^{20}Ne	4.33×10^{-3}	1.706×10^{-3}	1.206×10^{-3}	8.10×10^{-4}	5.78×10^{-4}	4.99×10^{-4}	4.14×10^{-4}	3.18×10^{-4}
^{21}Ne	1.136×10^{-5}	5.19×10^{-6}	3.90×10^{-6}	3.01×10^{-6}	2.56×10^{-6}	2.24×10^{-6}	1.970×10^{-6}	1.598×10^{-6}
^{22}Ne	3.48×10^{-4}	1.378×10^{-4}	9.79×10^{-5}	6.55×10^{-5}	4.83×10^{-5}	4.14×10^{-5}	3.41×10^{-5}	2.67×10^{-5}
^{36}Ar	5.40×10^{-4}	1.882×10^{-4}	1.269×10^{-4}	9.39×10^{-5}	5.89×10^{-5}	5.99×10^{-5}	6.04×10^{-5}	5.03×10^{-5}
^{38}Ar	1.015×10^{-4}	3.65×10^{-5}	2.49×10^{-5}	1.861×10^{-5}	1.187×10^{-5}	1.196×10^{-5}	1.231×10^{-5}	1.033×10^{-5}
^{40}Ar	1.193×10^{-3}	4.13×10^{-4}	2.78×10^{-4}	2.22×10^{-4}	1.333×10^{-4}	1.518×10^{-4}	1.599×10^{-4}	1.323×10^{-4}
^{84}Kr	2.51×10^{-7}	8.58×10^{-8}	6.15×10^{-8}	4.30×10^{-8}	3.02×10^{-8}	2.81×10^{-8}	2.94×10^{-8}	2.92×10^{-8}
^{132}Xe	6.4×10^{-8}	2.2×10^{-8}	1.47×10^{-8}	1.16×10^{-8}	7.12×10^{-9}	7.7×10^{-9}	7.8×10^{-9}	7.3×10^{-9}
^{4}He/^{3}He	2970	2800	2810	2540	2360	2370	2240	2350
^{20}Ne/^{22}Ne	12.44	12.38	12.32	12.37	11.97	12.05	12.14	11.91
^{22}Ne/^{21}Ne	30.6	26.6	25.1	21.8	18.87	18.48	17.31	16.71
^{36}Ar/^{38}Ar	5.32	5.16	5.10	5.05	4.96	5.01	4.91	4.87
^{40}Ar/^{36}Ar	2.21	2.19	2.19	2.36	2.26	2.53	2.65	2.63
^{4}He/^{20}Ne	62.6	57.7	59.8	53.5	55.0	57.1	49.5	57.9
^{20}Ne/^{36}Ar	8.02	9.06	9.50	8.63	9.81	8.33	6.85	6.32
^{36}Ar/^{84}Kr	2150	2190	2060	2180	1950	2130	2050	1720
^{84}Kr/^{132}Xe	3.9	3.9	4.2	3.7	4.3	3.6	3.8	4.0

reference soil 74241 have been published recently (Hintenberger and Weber, 1973, Tables 3 and 4). Some bulk samples have isotopic and elemental noble gas ratios outside the spread of values obtained in grain size fractions. Especially the ^{4}He/^{3}He, ^{20}Ne/^{22}Ne, and ^{4}He/^{20}Ne ratios tend to be higher in bulk samples. This effect is larger than the experimental error and could be attributable to gas losses or connected with the loss of very fine grained material during sieving. Experiments are planed to clarify this discrepancy.

Mineral separates

More detailed information can be anticipated from the investigation of mineral separates of known grain sizes. These investigations are in progress and therefore only a few preliminary results can be included in this paper. Up to now, we have measured the rare gases in the 35.5–54 μm ilmenite grain size fractions of 3 soils and a breccia from the Apollo 17 missions. These preliminary results are listed in Table 9.

DISCUSSION

In order to compare the concentration of trapped noble gases in different soils from Apollo 17 the isotopes ^{4}He, ^{20}Ne, ^{36}Ar, ^{84}Kr, and ^{132}Xe are plotted in Fig. 1. The samples are arranged from the top to bottom with decreasing ^{36}Ar-

Table 8. Rare gas concentrations in cm^3 STP/g in grain size fractions of breccia from Apollo 17 sample 79135,32. Errors in isotope ratios 2%, errors in concentrations of He, Ne, and Ar about 3%, of Kr and Xe about 10%. Sample weights between 0.6–2.1 mg.

	<5 μm	5–10 μm	10–20 μm	<20 μm	20–25 μm	25–35 μm	35–54 μm	54–75 μm	75–120 μm	120–200 μm
^{3}He	9.98×10^{-5}	4.96×10^{-5}	5.64×10^{-5}	8.70×10^{-5}	3.98×10^{-5}	3.29×10^{-5}	3.21×10^{-5}	1.203×10^{-5}	1.683×10^{-5}	3.38×10^{-5}
^{4}He	3.04×10^{-1}	1.463×10^{-1}	1.699×10^{-1}	2.63×10^{-1}	1.166×10^{-1}	9.52×10^{-2}	9.13×10^{-2}	2.67×10^{-2}	4.32×10^{-2}	9.77×10^{-2}
^{20}Ne	6.31×10^{-3}	3.31×10^{-3}	3.65×10^{-3}	5.36×10^{-3}	2.61×10^{-3}	2.20×10^{-3}	2.15×10^{-3}	6.76×10^{-4}	9.32×10^{-4}	2.35×10^{-3}
^{21}Ne	1.664×10^{-5}	9.03×10^{-6}	9.89×10^{-6}	1.430×10^{-5}	7.49×10^{-6}	6.68×10^{-6}	6.52×10^{-6}	3.07×10^{-6}	3.53×10^{-6}	6.82×10^{-6}
^{22}Ne	4.98×10^{-4}	2.66×10^{-4}	2.87×10^{-4}	4.26×10^{-4}	2.07×10^{-4}	1.764×10^{-4}	1.712×10^{-4}	5.53×10^{-5}	7.52×10^{-5}	1.863×10^{-4}
^{36}Ar	8.86×10^{-4}	4.27×10^{-4}	5.16×10^{-4}	8.76×10^{-4}	3.39×10^{-4}	3.42×10^{-4}	2.99×10^{-4}	8.68×10^{-5}	1.291×10^{-4}	3.89×10^{-4}
^{38}Ar	1.671×10^{-4}	8.09×10^{-5}	9.75×10^{-5}	1.692×10^{-4}	6.43×10^{-5}	6.62×10^{-5}	5.77×10^{-5}	1.748×10^{-5}	2.54×10^{-5}	7.43×10^{-5}
^{40}Ar	2.14×10^{-3}	1.007×10^{-3}	1.236×10^{-3}	2.19×10^{-3}	8.12×10^{-4}	8.53×10^{-4}	7.46×10^{-4}	2.23×10^{-4}	3.34×10^{-4}	9.56×10^{-4}
^{84}Kr	4.05×10^{-7}	1.94×10^{-7}	2.27×10^{-7}	3.79×10^{-7}	1.54×10^{-7}	1.45×10^{-7}	1.33×10^{-7}	4.43×10^{-8}	5.77×10^{-8}	1.90×10^{-7}
^{132}Xe	1.3×10^{-7}	6.5×10^{-8}	6.7×10^{-8}	1.1×10^{-7}	4.9×10^{-8}	3.7×10^{-8}	4.0×10^{-8}	1.2×10^{-8}	1.7×10^{-8}	5.2×10^{-8}
$^{4}He/^{3}He$	3050	2950	3010	3020	2930	2890	2840	2220	2570	2890
$^{20}Ne/^{22}Ne$	12.67	12.44	12.72	12.58	12.61	12.47	12.56	12.22	12.39	12.61
$^{22}Ne/^{21}Ne$	29.9	29.5	29.0	29.8	27.6	26.4	26.3	18.01	21.3	27.3
$^{36}Ar/^{38}Ar$	5.30	5.28	5.29	5.18	5.27	5.17	5.18	4.97	5.08	5.24
$^{40}Ar/^{36}Ar$	2.42	2.36	2.40	2.50	2.40	2.49	2.49	2.57	2.59	2.46
$^{4}He/^{20}Ne$	48.2	44.2	46.5	49.1	44.7	43.3	42.5	39.5	46.4	41.6
$^{20}Ne/^{36}Ar$	7.12	7.75	7.07	6.12	7.78	6.43	7.19	7.79	7.22	6.04
$^{36}Ar/^{84}Kr$	2190	2200	2240	2310	2200	2360	2300	1960	2240	2050
$^{84}Kr/^{132}Xe$	3.2	3.0	3.4	3.6	3.1	3.9	3.3	3.8	3.4	3.7

Table 9. Rare gas content and elemental ratios in bulk and ilmenite grain size fractions (35–54 μm) of Apollo 17 soils and breccias (cc STP/g^{-1}).

	Weight (mg)		^{4}He	^{20}Ne	^{36}Ar	^{4}He/^{36}Ar	^{20}Ne/^{36}Ar
72701,25	0.20	Ilm.	1.110×10^{-1}	5.75×10^{-4}	4.29×10^{-5}	2590	13.4
		Bulk	1.967×10^{-2}	4.77×10^{-4}	1.115×10^{-4}	176.4	4.28
		I/B	5.64	1.21	0.385	14.6	3.1
74241,24	0.56	Ilm.	9.61×10^{-2}	3.41×10^{-4}	1.284×10^{-5}	7480	26.6
		Bulk	2.18×10^{-2}	2.66×10^{-4}	2.38×10^{-5}	916	11.2
		I/B	4.41	1.28	0.539	8.18	2.4
75081,72	1.20	Ilm.	1.419×10^{-1}	6.67×10^{-4}	3.09×10^{-5}	4590	21.6
		Bulk	5.01×10^{-2}	6.81×10^{-4}	9.90×10^{-5}	506	6.88
		I/B	2.83	0.979	0.312	9.07	3.1
79035,15	1.00	Ilm.	1.224×10^{-1}	9.91×10^{-4}	8.61×10^{-5}	1420	11.5
		Bulk	4.33×10^{-2}	8.10×10^{-4}	9.39×10^{-5}	461	8.63
		I/B	2.83	1.22	0.917	3.09	1.33

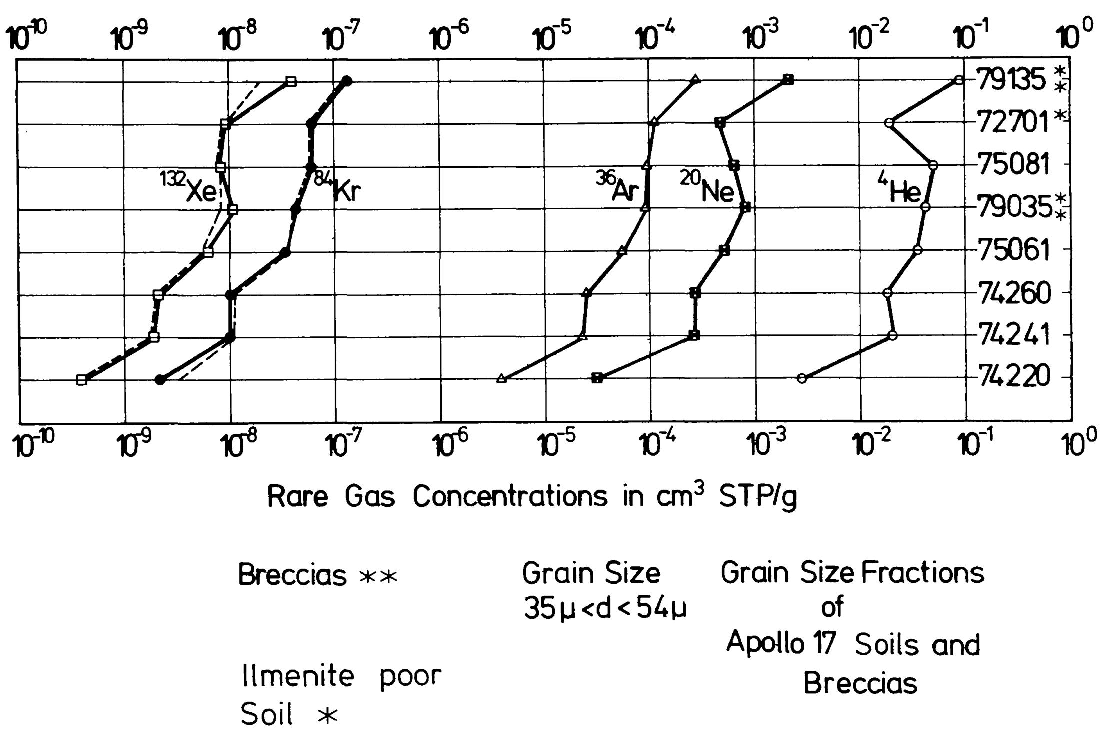

Fig. 1. Concentration of ^{4}He, ^{20}Ne, ^{36}Ar, ^{84}Kr, and ^{132}Xe in 35–54 μm grain size fractions of Apollo 17 soils and breccias. The dashed lines are parallel to the ^{36}Ar line. The low concentration of ^{4}He and ^{20}Ne in 72701 is explained by its low ilmenite content.

concentration. Hintenberger and Weber (1973) have used a similar diagram to compare trapped noble gas concentrations from different landing sites. Figure 1 is, however, modified with respect to the following points:

(1) The influence of different grain size distributions in the various soils has been eliminated by using only 35–54 μm grain size fractions.
(2) ^{36}Ar was taken as an indicator of the solar wind irradiation (i.e. the samples are arranged after decreasing ^{36}Ar concentration) because ^{36}Ar is normally more precisely determined than ^{84}Kr.

In Fig. 1 the lines for the heavy rare gases ^{36}Ar, ^{84}Kr, and ^{132}Xe of soils are parallel to each other, indicating constant ratios of ^{36}Ar/^{84}Kr and ^{36}Ar/^{132}Xe of 2100 ± 300 and 13400 ± 2000, respectively. The concentrations of trapped ^{36}Ar, ^{84}Kr, and ^{132}Xe in lunar samples can be taken—at least as an approximation—as indicators of solar wind exposure. Therefore, in Fig. 1 the samples suffered from top to bottom less and less solar irradiation. This sequence is the same for each of the three isotopes ^{36}Ar, ^{84}Kr, and ^{132}Xe. The ^{4}He and ^{20}Ne concentrations, however, would define completely different sequences, an effect which is understood in terms of diffusive losses of the light trapped rare gases. To become independent as far as possible from these losses, ^{132}Xe would be the best rare gas isotope as indicator of solar wind exposure. However, in Fig. 1 we prefered ^{36}Ar because of its smaller experimental error.

As noted by Eugster *et al.* (1972) and Hintenberger and Weber (1973), high ^{4}He/^{20}Ne and ^{20}Ne/^{36}Ar ratios in lunar soil samples are connected with high ilmenite contents. This holds also for Apollo 17 samples. The ^{20}Ne and the ^{4}He lines show a marked minimum for the light mantle soil 72701 which has the lowest ilmenite content (1.5% TiO_2) of all the samples in this diagram.

This indicates again a loss of the light rare gases ^{4}He and ^{20}Ne in ilmenite poor soils. Figure 2 demonstrates the correlation of the ratios ^{4}He/^{20}Ne and ^{20}Ne/^{36}Ar of the trapped rare gas nuclides with the concentrations of TiO_2 as a measure for the ilmenite content in the Apollo 17 soils and breccias investigated in this paper.

A more detailed inspection of Fig. 1 shows two maxima in the ^{132}Xe line for the two breccias 79035 and 79135 which indicate a ^{132}Xe excess as compared to ^{132}Xe calculated from the ^{36}Ar content. In the diagram of our Apollo 11 to Apollo 16 data (Hintenberger and Weber, 1973, Fig. 1) also the breccias 10021 and 10046 show distinct humps in the ^{132}Xe line. This feature is more clearly shown in Fig. 3, where the ^{132}Xe/^{36}Ar ratios versus the ^{36}Ar concentrations are plotted. We have included in this diagram also our data from the samples of earlier missions. Most soil samples show distinctly lower ^{132}Xe/^{36}Ar ratios than the breccias. Thus, the formation of a breccia is at least in many cases connected either with an incorporation of ^{132}Xe or with a loss of ^{36}Ar. Figure 4 shows the corresponding diagram for the ^{84}Kr/^{36}Ar ratio. An argon loss without a krypton loss would influence this ratio in a similar way as the ^{132}Xe/^{36}Ar ratio, but no systematic increase of the ^{84}Kr/^{36}Ar ratio in breccias is observed. Therefore, the high

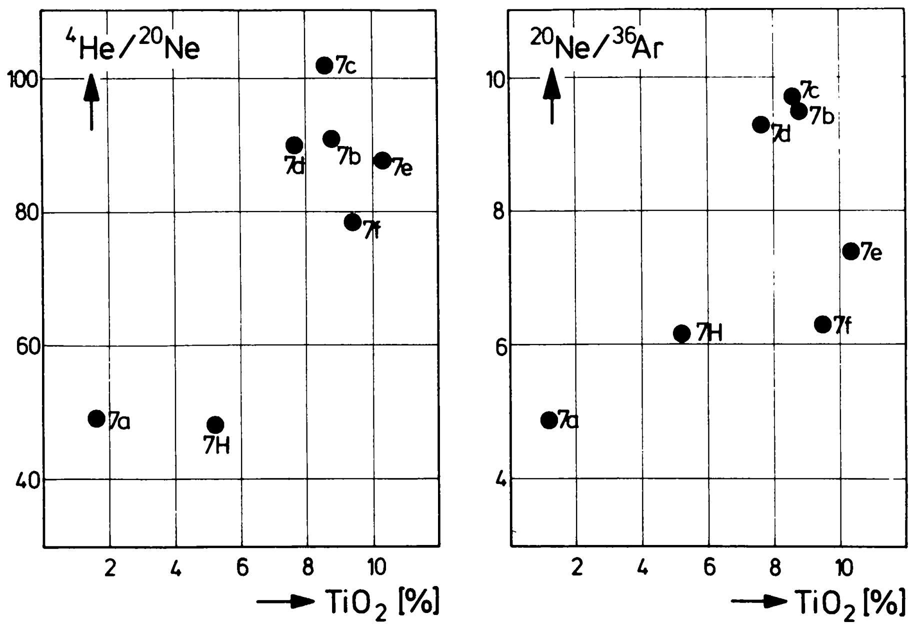

Fig. 2. Correlation between the TiO_2 contents and trapped rare gas ratios in Apollo 17 soils and breccias. TiO_2 is a measure of the ilmenite content of the sample. Numbers on points are explained in Table 1.

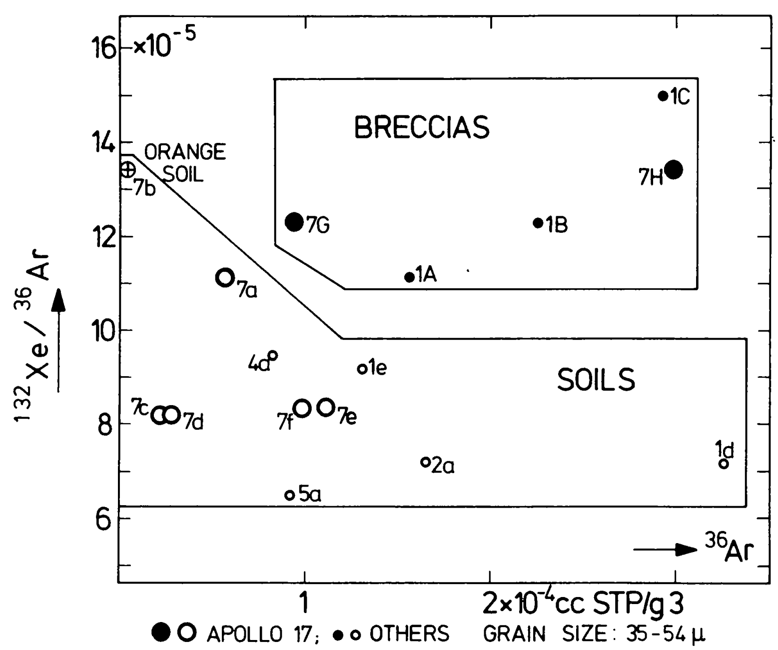

Fig. 3. $^{132}Xe/^{36}Ar$ as a function of trapped ^{36}Ar in Apollo 17 soils (large open circles) and breccias (large closed circles). For comparison measurements from other lunar missions are included. Grain size effects are excluded by taking for all samples the analyses of the same grain size fractions (35–54 μm). Numbers on points are explained in Table 1.

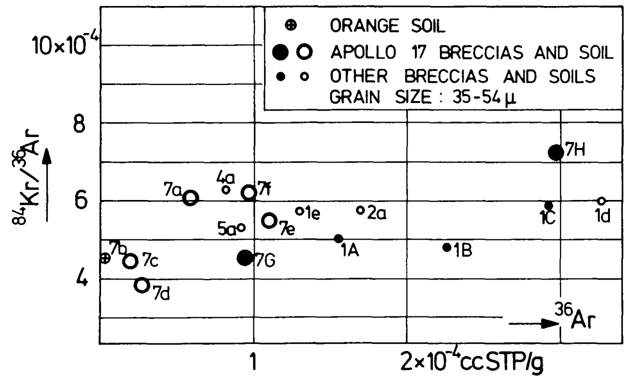

Fig. 4. $^{84}Kr/^{36}Ar$ as a function of ^{36}Ar in soils (open circles) and breccias (closed circles).

$^{132}Xe/^{36}Ar$ ratios in these breccias must be caused by an excess of trapped Xe, or a simultaneous loss of ^{36}Ar and ^{84}Kr.

The influence of the dose of solar wind irradiation on the $^{4}He/^{36}Ar$ and $^{20}Ne/^{36}Ar$ ratios can be seen from Fig. 5 and 6. The concentration of ^{36}Ar is taken as a measure of the total solar exposure. To reduce the influence of differences in the gas retentivities we have compared only the data obtained on ilmenite rich samples ($TiO_2 > 6\%$). Both ratios, $^{4}He/^{36}Ar$ as well as $^{20}Ne/^{36}Ar$, decrease systematically with increasing ^{36}Ar concentrations. This can be explained by an enhanced diffusive loss of ^{4}He and ^{20}Ne due to larger radiation damages in highly irradiated crystals. However, the same pattern would be expected if saturation effects as mentioned by Eberhardt *et al.* (1970) are responsible for the observed noble gas pattern in lunar soils. More detailed information on this subject can be

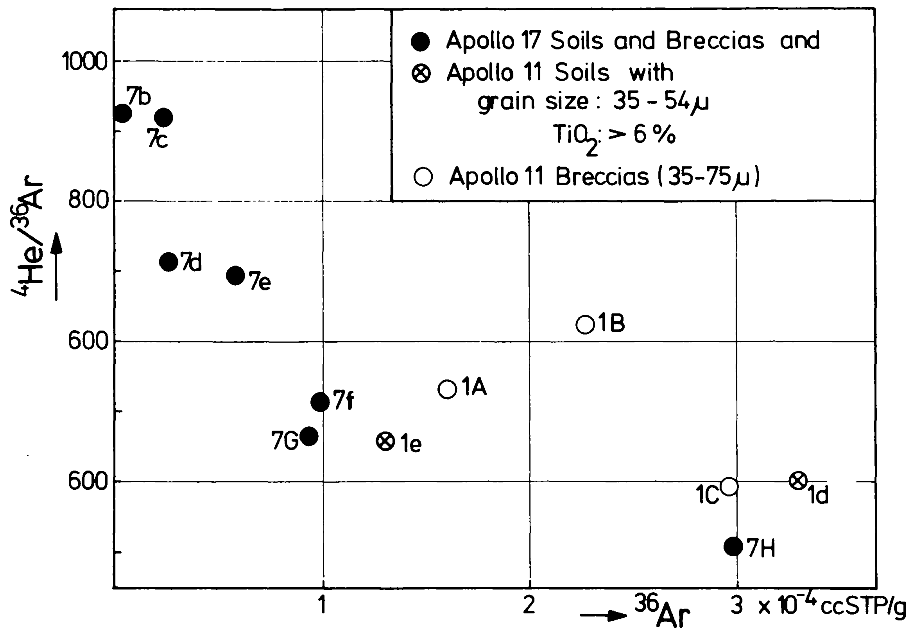

Fig. 5. $^{4}He/^{36}Ar$ versus ^{36}Ar in lunar soils and breccias. Only materials with TiO_2 contents larger than 6% are considered. Numbers on points are explained in Table 1.

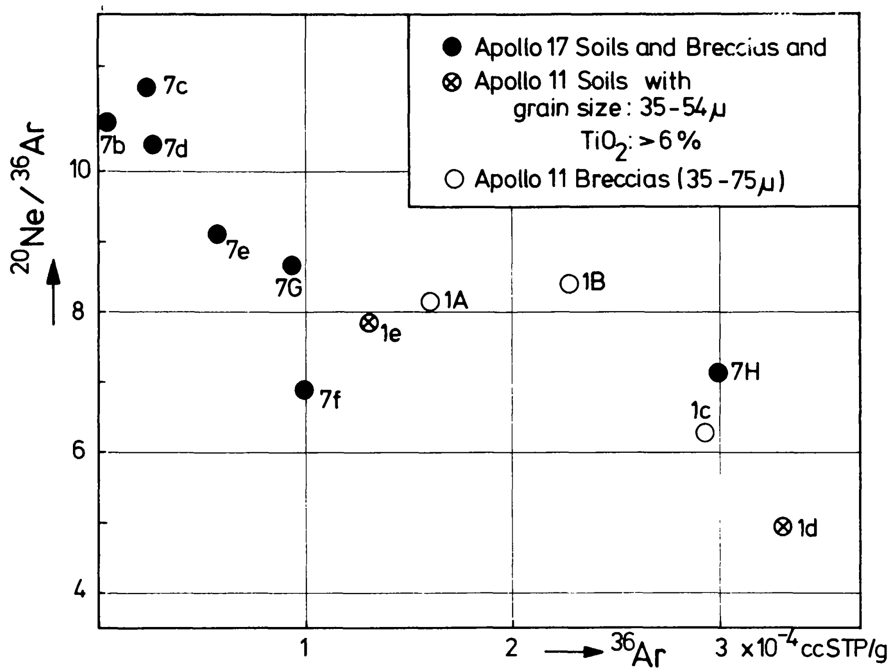

Fig. 6. $^{20}Ne/^{36}Ar$ versus ^{36}Ar in lunar soils and breccias.

obtained by the investigation of mineral fractions, first of all from the rare gas retentive ilmenite.

Figure 7 shows the concentrations of ^{4}He, ^{20}Ne, and ^{36}Ar in ilmenite normalized to the concentration of the same isotope in bulk material of the same grain size.

^{4}He and ^{20}Ne have higher concentrations in ilmenite. This reflects the high retentivity of implanted light noble gases in ilmenite (Eberhardt *et al.*, 1970). All three soils contain, however, more ^{36}Ar in the bulk material. This may imply different irradiation histories for bulk and ilmenite of the same soil. Eberhardt *et*

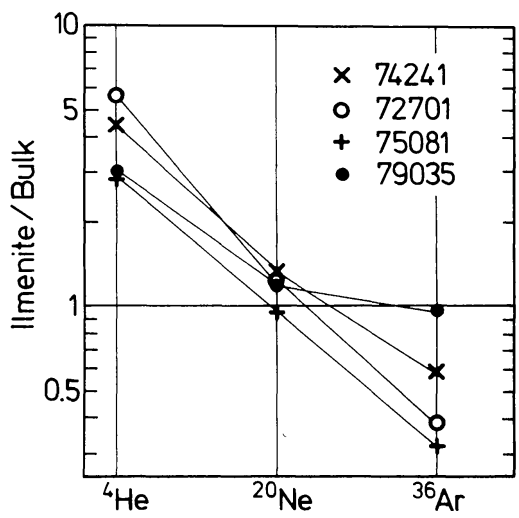

Fig. 7. Comparison of concentrations of ^{4}He, ^{20}Ne, and ^{36}Ar in ilmenite and bulk samples (grain size: 35–54 μm).

al. (1972) have shown that in 10084 and 12001 the cosmic ray exposure age of ilmenite is smaller than the exposure age of the bulk soil. Measurements on ilmenite of different grain sizes will be necessary to prove whether this explanation is also true for the Apollo 17 soils investigated here. It may be noted that the breccia 79035 has about the same concentration of trapped ^{36}Ar in ilmenite and bulk samples.

Besides the surface correlated trapped component, lunar soils and breccias contain volume correlated spallogenic and radiogenic noble gases. A separation of these components is possible if grain size fractions are analyzed (Eberhardt *et al.*, 1970; Heymann and Yaniv, 1970; Hintenberger *et al.*, 1970b, 1971; Hintenberger and Weber, 1973). This method has been used to determine the radiogenic ^{40}Ar concentration. Figure 8 shows ^{40}Ar correlation plots for Apollo 17 soils and breccias. The radiogenic ^{40}Ar is given by the ordinate intercept; the ratio of the surface correlated argon components $(^{40}Ar/^{36}Ar)_{SC}$ is given by the slope of the line. The method assumes that radiogenic ^{40}Ar is the same in all grain size fractions.

Table 10 contains the results for radiogenic ^{40}Ar and K–Ar ages, calculated with K values from Table 1. For the soils 72701 and 74220, and to some extent also for 75061 and 75081, the correlation lines of Fig. 8 can be used to determine the radiogenic and the surface correlated ^{40}Ar components with relatively small errors. The two reference soils 74241 and 74260, however, as well as the breccias 79035 and 79135 contain very high amounts of surface correlated ^{40}Ar. In such cases, correlation plots cannot resolve the surface and volume correlated components. Therefore, we can give only upper limits for the K–Ar ages of these soils. These limits are higher than our recently published results for 74241 (Hintenberger and Weber, 1973) due to a computational error. The difference in age between the orange soil and the adjacent gray soil has become smaller and—considering the difficulties in resolving the two components—does not appear significant.

Table 10 also includes isotopic ratios of surface correlated gases and concentrations of volume correlated spallogenic nuclides (^{3}He, ^{21}Ne, ^{38}Ar).

The ratio $^{40}Ar/^{36}Ar$ of the surface correlated argon show a large range from 0.77 in 75081 to 7.6 in 74241. The ratio $^{4}He/^{3}He$ of the surface correlated helium isotopes shows a range from 2740 to 3260 in the corresponding samples. Geiss (1973) pointed out that these two ratios seem to be correlated. This is supported by our new results on the Apollo 17 samples (see Fig. 9). Geiss attempted to explain the correlation by a decrease of solar wind $^{4}He/^{3}He$ ratio with time combined with an enhanced ^{40}Ar retrapping from the moon's atmosphere at earlier times (Yaniv and Heymann, 1972). Such a correlation could, however, also be obtained if radiogenic ^{4}He and ^{40}Ar released from the moon's interior is adsorbed and partly incorporated into the highly damaged grain surfaces.

For the lunar regolith with a rather continuous mixing, a correlation between surface correlated gases in the grains incorporated at the very surface of the regolith and spallogenic gases produced in the top layer ($\sim$1 m) is expected. Figures 10 and 11 show the concentrations of trapped $(^{20}Ne)_{tr}$ and $(^{36}Ar)_{tr}$ versus spallogenic $(^{21}Ne)_{sp}$ in soils and breccias. Indeed, a correlation between trapped

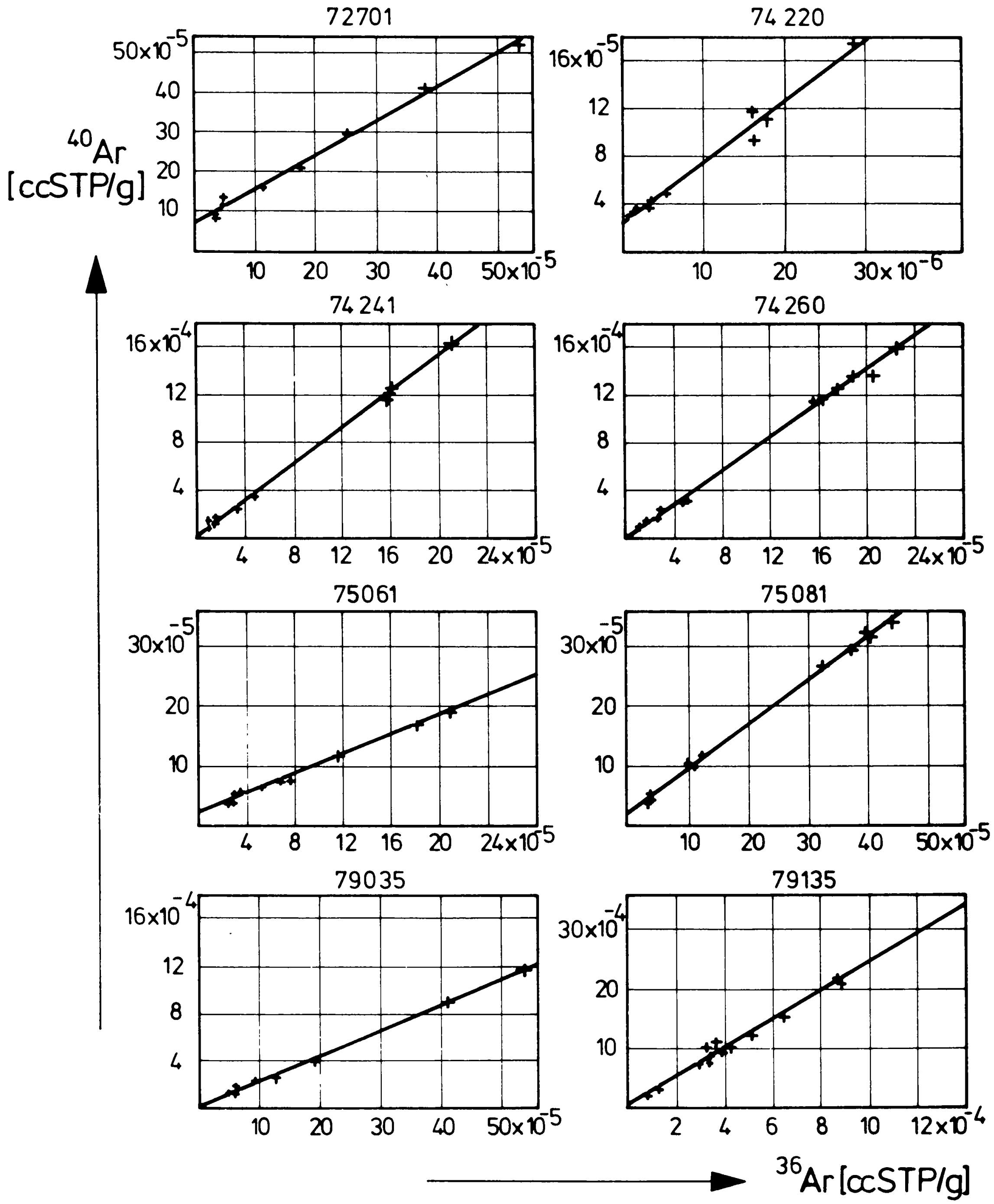

Fig. 8. ^{40}Ar versus ^{36}Ar in grain size fractions of Apollo 17 samples. The ordinate intercept determines the amount of radiogenic ^{40}Ar, the slope of the line the surface correlated ^{40}Ar/^{36}Ar ratio (see Table 10). The radiogenic ^{40}Ar cannot be deduced from such diagrams in cases of high surface correlated ^{40}Ar concentrations (74241, 74260, 79035, 79135). Similar diagrams have been used to compute the spallogenic isotopes given in Table 10.

Table 10. Concentrations (cm^3 STP/g) and isotope ratios of trapped, spallogenic and radiogenic rare gas nuclides of lunar fines and breccias.

	$\left(\frac{^4He}{^3He}\right)_{tr}$	$\left(\frac{^{20}Ne}{^{21}Ne}\right)_{tr}$	$\left(\frac{^{22}Ne}{^{21}Ne}\right)_{tr}$	$\left(\frac{^{36}Ar}{^{38}Ar}\right)_{tr}$	$\left(\frac{^{40}Ar}{^{36}Ar}\right)_{tr}$	$^3He_{sp}$	$^{21}Ne_{sp}$	$^{38}Ar_{sp}$	$^{40}Ar_{rad}$	^{21}Ne* Exposure age	K-Ar† age
						10^{-8} cm^3 STP/g				10^6 yr	10^9 yr
72701,25	2900 ±40	417 ±9	32.4 ±0.7	5.38 ±.04	0.89 ±.05	68 ±15	34 ±4	50 ±30	6700 ±1000	210 ±20	3.85 ±.25
74220,47	2970 ±40	399 ±4	30.8 ±0.3	5.26 ±0.06	5.2 ±0.2	15 ±2	4.3 ±0.2	2.6 ±1.3	2600 ±300	27 ±1	3.44 ±.17
74241,24	3260 ±50	411 ±4	32.8 ±0.4	5.20 ±0.04	7.4 ±0.3	120 ±21	25 ±2	24 ±5	≤2100	160 ±10	—
74260,9	3090 ±40	411 ±5	32.7 ±0.4	5.27 ±0.03	7.0 ±0.2	100 ±30	32 ±3	30 ±3	≤2100	200 ±20	—
75061,21	2770 ±50	413 ±12	32.1 ±.8	5.29 ±.03	0.85 ±.04	120 ±30	33 ±6	22 ±8	1800 ±400	210 ±40	3.0 ±.3
75081,72	2760 ±30	413 ±5	32.3 ±0.5	5.33 ±0.02	0.78 ±0.02	110 ±30	37 ±4	53 ±11	1800 ±300	230 ±20	2.9 ±.2
79035,15	2980 ±60	409 ±8	32.5 ±.7	5.32 ±.03	2.18 ±.05	220 ±50	96 ±8	100 ±15	1700 ±700	600 ±50	2.5 ±.5
79135,32	3170 ±20	423 ±8	33.0 ±.5	5.29 ±.03	2.5 ±.1	305 ±25	130 ±10	100 ±40	—	810 ±60	—

*Calculated with a production rate of 0.16×10^{-8} cc STP g^{-1} m.y.$^{-1}$.
†K values from Table 1. For 79035 a K concentration of 830 ppm was used.

and spallogenic rare gases is observed. The following relations hold for all concentrations obtained on 35–54 μm fractions of soils and breccias listed in Table 1, two additional Apollo 17 soils (74220 and 74241) as well as three Apollo 11 breccias 10021, 10046, 10061, and five soils from earlier missions analyzed in our

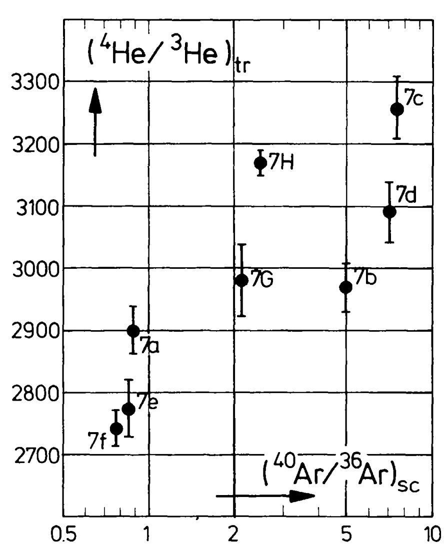

Fig. 9. Correlation of trapped ^{4}He/^{3}He and surface correlated ^{40}Ar/^{36}Ar in Apollo 17 materials. Numbers on points are explained in Table 1.

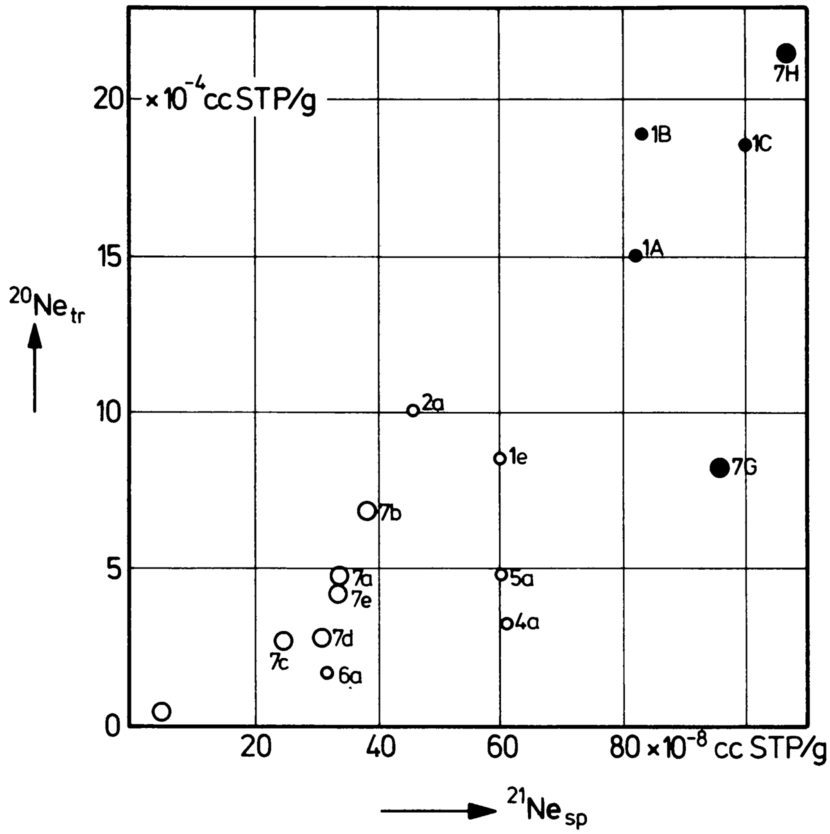

Fig. 10. Correlation of trapped ^{20}Ne in the 35–54 μm grain size fraction with spallogenic ^{21}Ne in Apollo 17 soils (large open circles) and breccias (large filled circles). For comparison data obtained in our laboratory from other lunar missions are included. The abbreviations used are explained in Table 1.

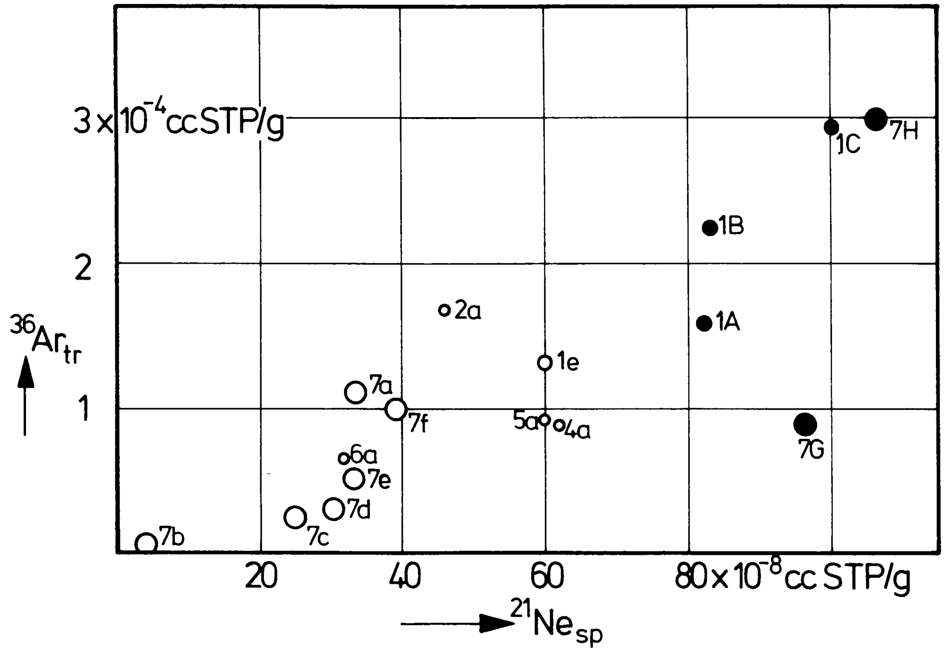

Fig. 11. Trapped ^{36}Ar versus spallogenic ^{21}Ne (see caption of Fig. 10). Numbers on points are explained in Table 1.

laboratory:

$$({}^{20}Ne)_{tr} \leq 2.3 \times 10^3 \times ({}^{21}Ne)_{sp}$$
$$({}^{36}Ar)_{tr} \leq 380 \times ({}^{21}Ne)_{sp}$$

In a very simplified model, one may explain these relations as valid for soils with continuous mixing. The deviations of data from this correlation may be due to a diffusion loss of ^{20}Ne or ^{36}Ar, or by an interruption of the solar wind exposure by an inhomogeneous mixing or by formation of a breccia.

An explanation for the extremely low $({}^{20}Ne)_{tr}$ and $({}^{36}Ar)_{tr}$ concentration together with the relatively high $({}^{21}Ne)_{sp}$ content of the breccia 79035 (Figs. 10 and 11) seems to be that about one-half of the spallogenic gases is produced before compaction and the other half after excavation of this rock. The use of such a plot could help to decipher the complex irradiation history of some lunar breccias. However, a larger number of different breccias and soils have to be analyzed to demonstrate that it is really possible to draw conclusions on the exposure time of lunar breccias from correlation diagrams like Figs. 10 and 11.

Acknowledgments—We are grateful to NASA for generously providing the lunar samples. We thank Mrs. Chr. Reitz for technical assistance.

REFERENCES

Baur H., Frick U., Funk H., Schultz L., and Signer P. (1972) On the question of retrapped ^{40}Ar in lunar fines (abstract). In *Lunar Science—III*, pp. 47–49. The Lunar Science Institute, Houston.

Eberhardt P., Geiss J., Graf H., Grögler N., Krähenbühl U., Schwaller H., Schwarzmüller J., and Stettler A. (1970) Trapped solar wind noble gases, exposure age and K/Ar-age in Apollo 11 lunar fine material. *Proc. Apollo 11 Lunar Sci. Conf., Geochim. Cosmochim. Acta*, Suppl. 1, Vol. 2, pp. 1037–1070. Pergamon.

Eberhardt P., Geiss J., Graf H., Grögler N., Mendia M. D., Mörgeli M., Schwaller H., and Stettler A. (1972) Trapped solar wind noble gases in Apollo 12 lunar fines 12001 and Apollo 11 breccia 10046. *Proc. Third Lunar Sci. Conf., Geochim. Cosmochim. Acta*, Suppl. 3, Vol. 2, pp. 1821–1856. MIT Press.

Eugster O., Grögler N., Mendia M. D., Eberhardt P., and Geiss J. (1973) Trapped solar wind noble gases and exposure age of Luna 16 lunar fines. *Geochim. Cosmochim. Acta* **37**, pp. 1991–2003.

Frick U., Baur H., Funk H., Phinney D., Schäfer Chr., Schultz L., and Signer P. (1973) Diffusion properties of light noble gases in lunar fines. *Proc. Fourth Lunar Sci. Conf., Geochim. Cosmochim. Acta*, Suppl. 4, Vol. 2, pp. 1987–2002. Pergamon.

Geiss J. (1973) Solar wind composition and implications about the history of the solar system. Preprint.

Heymann D. and Yaniv A. (1970) Inert gases in the fines from the Sea of Tranquillity. *Proc. Apollo 11 Lunar Sci. Conf., Geochim. Cosmochim. Acta*, Suppl. 1, Vol. 2, pp. 1247–1259. Pergamon.

Hintenberger H. and Weber H. W. (1973) Trapped rare gases in lunar fines and breccias. *Proc. Fourth Lunar Sci. Conf., Geochim. Cosmochim. Acta*, Suppl. 4, Vol. 2, pp. 2003–2019. Pergamon.

Hintenberger H., Weber H. W., Voshage H., Wänke H., Begemann F., and Wlotzka F. (1970) Concentrations and isotopic abundances of the rare gases, hydrogen, and nitrogen in Apollo 11 lunar matter. *Proc. Apollo 11 Lunar Sci. Conf., Geochim. Cosmochim. Acta*, Suppl. 1, Vol. 2, pp. 1269–1282. Pergamon.

Hintenberger H., Weber H. W., and Takaoka N. (1971) Concentrations and isotopic abundance of the rare gases in lunar matter. *Proc. Second Lunar Sci. Conf., Geochim. Cosmochim. Acta*, Suppl. 2, Vol. 2, pp. 1607–1625. MIT Press.

Hoffman J. H., Hodges R. R., and Johnson F. S. (1973) Lunar atmospheric composition results from Apollo 17. *Proc. Fourth Lunar Sci. Conf., Geochim. Cosmochim. Acta*, Suppl. 4, Vol. 3, pp. 2865–2875. Pergamon.

Jovanovic S. and Reed G. W., Jr. (1974) Labile trace elements in Apollo 17 samples (abstract). In *Lunar Science—V*, pp. 391–393. The Lunar Science Institute, Houston.

LSPET (Lunar Sample Preliminary Examination Team) (1973) Apollo 17 Lunar Samples: Chemical and Petrographic Description. *Science* **182**, 659–671.

Morgan J. W., Ganapathy R., Higuchi H., Krähenbühl U., and Anders E. (1974) Lunar basins: Tentative characterization of projectiles, from meteorite elements in Apollo 17 boulders (abstract). In *Lunar Science—V*, pp. 526–528. The Lunar Science Institute, Houston.

Nunes P. D., Tatsumoto M., and Unruh D. M. (1974) U–Th–Pb systematics of some Apollo 17 samples (abstract). In *Lunar Science—V*, pp. 562–564. The Lunar Science Institute, Houston.

Schultz L. and Hintenberger H. (1967) Edelgasmessungen an Eisenmeteoriten. *Zs. Naturf.* **22a**, pp. 773–779.

Tatsumoto M., Nunes P. D., Knight R. J., Hedge C. E., and Unruh D. M. (1973) U–Th–Pb, Rb–Sr, and K measurements of two Apollo 17 samples. *EOS* **54**, 614–615.

Weber H. (1973) Thesis. Johannes Gutenberg-Universität, Mainz.

Yaniv A. and Heymann D. (1972) Atmospheric Ar^{40} in lunar fines. *Proc. Third Lunar Sci. Conf., Geochim. Cosmochim. Acta*, Suppl. 3, Vol. 2, pp. 1967–1980. MIT Press.